Impact damages detection on composite materials by THz imaging

Fabien Destic, Christophe Bouvet

Impact damages detection on composite materials by THz imaging

Fabien Destic [a,*], Christophe Bouvet [a,b]

[a] Institut Supérieur de l'Aéronautique et de l'Espace (ISAE-SUPAERO), Université de Toulouse, 31055 Toulouse Cedex 4, France
[b] Institut Clément Ader (ICA), Université de Toulouse, CNRS, INSAT, ISAE-SUPAERO, Mines Albi, UPS, 31077 Toulouse Cedex 4, France

A B S T R A C T

This paper presents a Non-Destructive Testing (NDT) method based on the penetration properties of terahertz (THz) waves. A CW raster-scanning THz imaging setup, using a 3.8 THz Quantum Cascade Laser as a source, is used to perform NDT of polypropylene/polypropylene composite samples.
Results from transmission and reflection THz imaging are compared to ultrasound C-scan. THz images in reflection give similar results to C-scan whereas THz transmission images provide more information about delaminations and cracks in the fiber fabrics.

1. Introduction

The field of THz waves lies in the electromagnetic spectrum in the frequency range between 300 GHz and 10 THz, or in wavelengths from 30 µm to 1 mm. On the one hand, the energy of THz photons is very low, below 40 meV. On the other hand, most non-metallic and non-polar media are "transparent" to THz waves. These two properties make THz waves a potential candidate for Non-Destructive Testing in a variety of fields, such as art conservation science [1], plastic weld joints [2], quality control on chocolate bars [3] or the absorption of water into polyamide and wood plastic composite [4].

A composite material is a combination of two (or more) materials working together that give the composite its unique properties. This denomination is applied to many materials and many sectors: glass, aramide or carbon fibre reinforced composites used in the aeronautics and automotive industries or sports equipment, and wood composite in furniture manufacturing, among others.

NDT using THz waves can be an alternative when "traditional" methods are not very efficient (composite made from soft epoxy resin, for instance) or to improve spatial resolution. In a simplified manner, there are two kinds of THz radiation technology: pulsed and Continuous Wave (CW).

In pulsed systems, a femtosecond Ti:Sa or mode-locked fiber laser (duration ~100 fs) produces an optical-pulse train sent on a THz emitter (photoconductive antenna or nonlinear crystal) to form electromagnetic pulses. After being transmitted through or reflected by the sample, the resulting waveform is coherently detected in time-domain using a delay line and Fourier Transformed to be analyzed in the frequency domain, providing a broad spectrum that covers typically the frequency range [0.1–3] THz [5].

* Corresponding author.
E-mail address: fabien.destic@isae.fr (F. Destic).

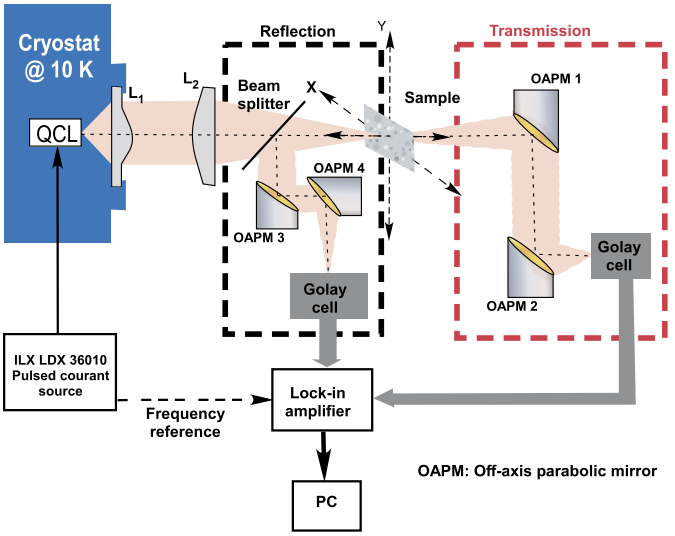

Fig. 1. Experimental setup.

The family of CW or quasi-CW systems can be divided into two types depending on the detection used: coherent detection, generally used with low power tunable sources, also uses an optical delay line and has the same characteristics as pulsed systems, and direct detection where phase information is not available but operations are faster and easier.

Over the past ten years, some research has been conducted on characterization or imaging, in the THz range, of various composite materials, most of which use pulsed THz-Time Domain Spectroscopy systems (THz-TDS). For instance, THz-NDT have been applied to titanium nanospheres in low density polyethylene (LDPE) [6] and glass-fibre reinforced polymers [7,8]. Fire damage testing on carbon or glass fibre was also explored [9–11]. The European FP7 project, DOTNAC, is dedicated to the development of a TDS setup to inspect aeronautics composite materials. Defects on glass fiber reinforced plastics (foreign material inserts, delaminations, or moisture contamination) can be visualized or coatings analyzed on carbon fiber samples [12]. Amenabar et al. propose a review to THz Non-Destructive Testing of composite matter [13].

Continuous wave THz inspection is also possible as demonstrated on sprayed-on foam insulation (SOFI) with a gas laser at 1.63 THz [9] or carbon fibre at 0.6 THz with Gunn diodes [10]. Composite materials diagnostic using CW THz waves produced by Quantum Cascade Laser on thin samples of glass fibre or Kevlar composite have been studied [14]. This approach seems to be very promising as QCLs are THz sources emitting a few tens of mW, at frequencies in the [1–4] THz range, with a constantly improving beam quality.

2. Experimental setup

The raster-scanning imaging experimental setup (Fig. 1) uses a 3.8 THz ($\lambda = 79$ µm) Quantum Cascade Laser (QCL) as a THz source. The laser, based on the Resonant-Phonon depopulation scheme, has been designed by R. Colombelli's group at Université Paris-Sud [15]. When cooled at $\sim$ 10 K by a closed cycle cryocooler, it emits 35 mW peak power in pulsed operation [16]. An ILX Lightwave LDX-36010-35 pulsed current source drives the QCL at 1.4 A by 950 µs long pulses at a 21 Hz repetition rate.

L_1 is a TPX lens that works both as a lens and a cryostat window. The collimated laser beam diameter is $\sim$13 mm in horizontal and $\sim$15 mm in vertical, divergence being $\sim$5 mrad. A second TPX lens, L_2, is used to focalize the laser beam in a 800 µm diameter spot where the sample under test is placed. The average power is $\sim$130 µW.

The sample to be imaged is moved in X and Y by two Newport SMC100 motorized translation stages. The setup can operate either in transmission mode with the off-axis parabolic mirrors inside the red dotted rectangle or in reflection mode by means of a HRFZ-Si beam splitter and mirrors in the black dotted rectangle. At each point or pixel, the mean and standard deviation of 10 intensity values from the detector (Tydex Golay cell, NEP = 113 pW.Hz$^{-1/2}$) is acquired via a Signal Recovery 7270DSP lock-in amplifier and, so, a transmission or reflection image can be constructed. Using a metallic resolution target, a spatial resolution of 0.5 mm in vertical and horizontal has been measured for the two arrangements of the imaging setup. The acquisition of a 30 mm $\times$ 30 mm image with 0.5 mm steps lasts about 1 h 25 min.

In order to characterize the THz images as objectively as possible, we will use two figures of merit:

- the dynamic range,

$$DR = 10.\log\left(\frac{Max}{min}\right)$$

where Max and min are the maximum and the minimum amplitude values in the image

- the signal-to-noise ratio,

$$SNR = 10.\log\left(\overline{\left[\frac{S_{i,j}}{N_{i,j}}\right]}\right)$$

where $S_{i,j}$ and $N_{i,j} = \sigma(S_{i,j})$ are the signal amplitude and the noise at pixel (i, j).

3. Impact damage detection

3.1. Samples

The samples used to demonstrate damage detection were 3 mm thick polypropylene composite plates, commercialized by Goodfellow under reference PP403300. This kind of composite has applications in automotive components, industrial cladding, audio products, personal protective equipment and sports goods.

The composite deals with 3 mm thickness plate manufactured from 20 woven plies oriented at 0° of thermoplastic self-reinforcing composite produced by compacting polypropylene fabric. This type of composite possesses a unique combination of impact/crash resistance and stiffness/strength. The density is 0.92 g/cm^3, the tensile modulus 5.0 GPa and the tensile stress is 180 MPa. In self-reinforced composite, the polymer matrix is reinforced with high-tenacity fibers of the same polymer family: in the present case, it deals with PP matrix and PP fibers. During the hot compacting manufacturing process, part of the fibers are melted and recrystallized upon cooling to bond the structure together. The global morphology of the obtained composite is not as clear as a classical composite with well separated plies, and, consequently, the resulting impact damage does not consist in delamination and matrix cracking (Fig. 2(c)) but rather in a damaged zone including matrix cracking and fiber/matrix debonding.

3.2. Damage creation

Fig. 2(a) shows the falling weight impact testing system used. The falling weight (mass = 2.03 kg) is in free fall guided in a tube. The impact energy is known from the velocity, measured by sensors [17]. Two 100 mm × 150 mm plates (Fig. 2(b)) have been impacted, in their center, with energies at levels of 10 J (sample S1) and 20 J (sample S2). The impact damage (Fig. 2(c)) consists of:

- dent depth due to the impactor contact
- matrix cracking
- delamination (failure of interface between consecutive plies)
- failure of the ply located back side

Of course, the higher the impact energy level, the greater the damage.

4. Results

4.1. Reflection THz imaging

For both samples, a reflection image is acquired with the setup and conditions described in Fig. 2. For each sample, S1 and S2, two images are taken: one with the sample illuminated on the impact side, so-called front side or recto, one illuminating the sample opposite to the impact i.e. back side or verso. The THz images are then compared to ultrasonic maps from a Krautkramer USD30 equipment. To perform these maps, called C-scan images, the plate is fully immersed in water. A single transducer of 3 MHz frequency (∼500 μm in wavelength) operating as a transmitter–receiver is scanned in a plane parallel to the composite plate surface and only the reflection from the back face is monitored. This technique allows to measure both the amplitude of the reflection and the time of flight, i.e. the time which is needed for an emitted pulse reflected from the back face of the sample to the receiver, and then to evaluate the depth of the first damage. As our setup does not give phase information, the amplitude C-scan ultrasounds images are compared to the THz reflection images (after converting intensity to amplitude). On all images, amplitude is normalized relative to its maximum and displayed on a color scale.

For each sample, paired images are shown and compared: THz reflection image and ultrasonic amplitude C-scan, sorted according to illumination side and impact energy.

In order to easily compare the images obtained with THz and C-scan techniques, the damage was highlighted with a dotted white form and the impact location was highlighted with an arrow (Figs. 3–7). Of course the damage form was the same for every image of the same impact, and symmetry was done for verso observations (Figs. 5–7). The sole purpose of the damage form was to compare the damage obtained with the different observations but it cannot be considered as the

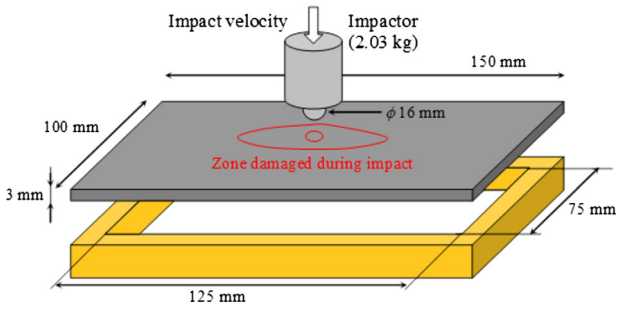

(a) Falling weight impact testing system (from [17])

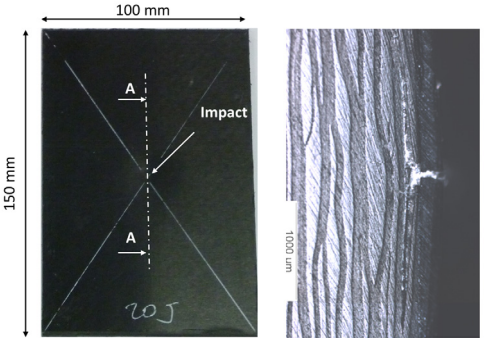

(b) Sample S2 showing dimensions and impact location (left) and microscope view of the A-A cut (right)

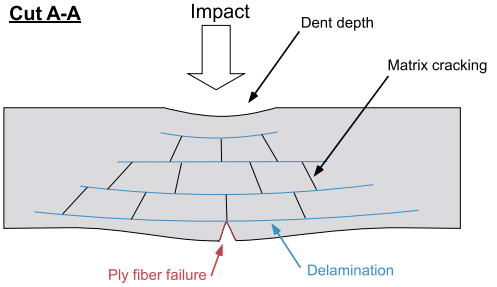

(c) Schematic cut of impact damage

Fig. 2. Damage creation.

exact damaged zone. In fact, the complementarity of the different observations was used in order to plot the damaged zone as accurately as possible.

4.1.1. Recto

Regarding the damage created on sample S1 by the 10 J impact (Fig. 3), the overall size of the observed damage zones is similar. In the THz image (Fig. 3(a)), the central spot, corresponding to the impact point, shows the maximum amplitude signal, while it is the most damaged zone. It is probably due to the dent depth created by the impactor (Fig. 2(c)), which may act as a concave reflector and as a light focalizer.

Fig. 4 summarizes the results obtained on the plate impacted with an energy of 20 J. The THz image (Fig. 4(a)) shows no significant difference with Fig. 3(a), corresponding to the 10 J impact. Indeed, in both cases, the damage area is expressed by a maximum signal located within a circle of 3–4 mm diameter which is probably due to the dent depth of the impactor in the “soft” material and, so, the creation of a concave reflector that may act as a light focalizer. There is not any significant size difference on the blue crescent-shaped areas (signal minimum). In the ultrasonic image Fig. 4(b), the damage is contained within a zone of 20 mm high and 15 mm wide. Within this zone, three maximum spots are seen. They are assumed to correspond to non-damaged areas, which seems unlikely regarding their locations and sizes. Rather they are probably measurement artifacts

Finally, for both the THz image and for the C-scan image, the observed damage zones are difficult to interpret.

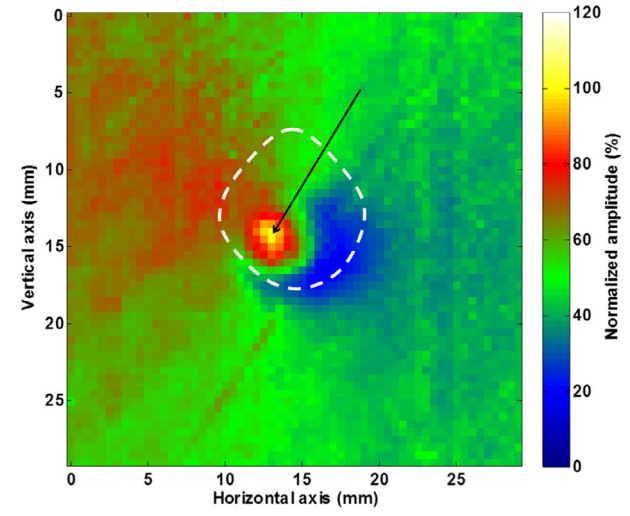

(a) THz reflection image

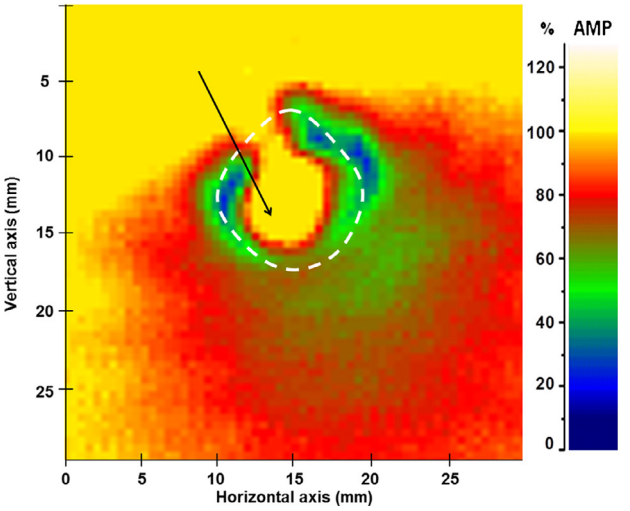

(b) Ultrasonic C-scan

Fig. 3. Sample S1 recto.

4.1.2. Verso

Results for the back side or verso observations are reported in Fig. 5 and Fig. 6 for the 10 J and 20 J impacts, respectively. In all cases, the verso observations are clearer than recto observations, for both THz and for ultrasonic investigations. This is most likely due to due to the shape of the back side which is less deformed than the front side. Indeed the dent depth left by the impactor at the front side probably disturbs the wave penetration in the plate. At the back side, in spite of the ply failure (Fig. 2(c) and Fig. 8), the plate shape is smoother.

At the two impact energies, the signal levels (eq. colors), shapes and sizes produced either by the THz setup or the ultrasound C-scan are quite similar: an elliptical blue–green zone corresponding to a low signal for sample S1 in the 10 J impact case (Fig. 5(a) and Fig. 5(b)), a “potato-like” zone for sample S2 in the 20 J case. But, both for 10 J impact and for 20 J impact, the damaged zone evaluated using THz investigation seems clearer than with the ultrasonic one.

4.2. Transmission THz imaging

Then, a transmission image is acquired for both samples. The sample is illuminated by the QCL on the recto. The average attenuation due to sample absorption and reflectance is about 30 dB.

Fig. 7(a) shows the resulting image for sample S1, impacted at 10 J. It presents a transmission minimum (red and brown) in an area of about 2 mm wide and 7 mm long (dimensions are determined from the intensity profile, not shown here). It corresponds to a non-impacted side crack, caused by the traction, which follows the weaving pattern. This crack, in the thickness of the plate, can be likened to a slot that diffracts terahertz radiation thus the signal is reduced. In the case of

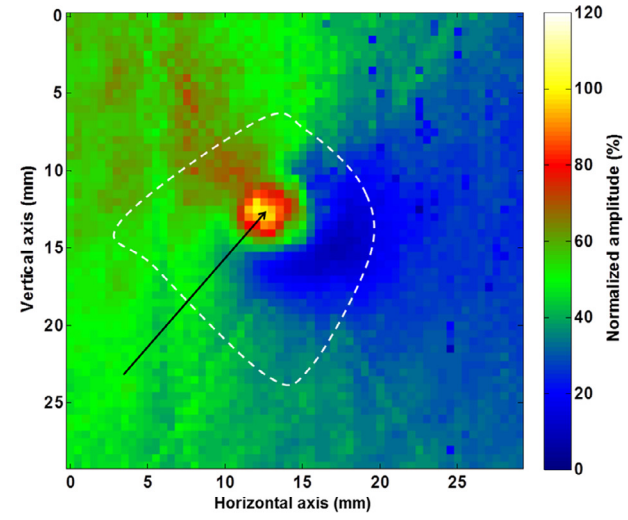

(a) THz reflection image

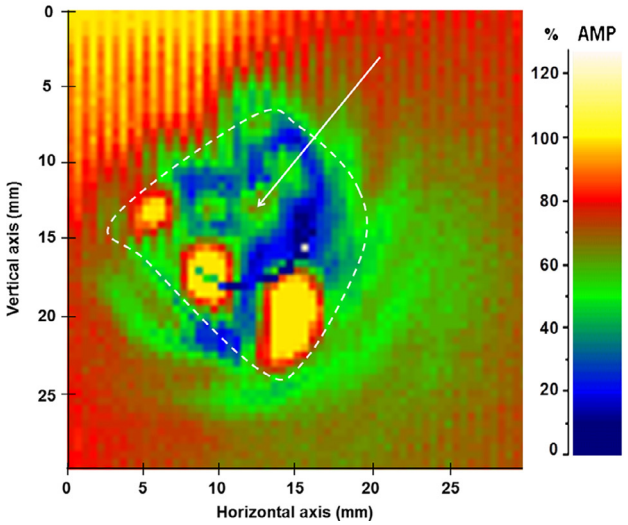

(b) Ultrasonic C-scan

Fig. 4. Sample S2 recto. (For interpretation of the references to color in this figure, the reader is referred to the web version of this article.)

sample S2 i.e. 20 J impact energy (Fig. 7(b)), the transmission image shows two perpendicular slots whose dimensions are approximately 11 mm wide and 10 mm high, corresponding to two cracks at 90° angle by the weave directions.

4.3. Considerations about THz images

Uncertainties are difficult to evaluate. In fact, the C-scan is a very classic method which is used here as the reference. Unfortunately, in this case, the C-scan of woven PP composite gives uncertain results. This is most probably due to the complex morphology of the impact damage due to the hot compacting manufacturing process which melts the fibers of consecutive plies together.

Table 1 summarizes the DR and SNR obtained for the different THz images. On the one hand, dynamic range is higher for reflection images (∼19–20 dB) than for transmission, probably due to the shape of samples. For recto illumination, the dent depth of the impactor focalize the reflected light and the signal is high. Recto illumination were also used for transmission images but in these cases, the light is absorbed and diffracted during propagation through the material. In the damaged zone, diffraction effects are much higher and so, the signal intensity is lower.

On the other hand, SNR is better for transmission than for reflection experiments. This behavior is a result of the lock-in amplifier response to signal dynamic range: given that the amplifier input range is fixed regarding the high level, then the low level signal measurement is noisier and the SNR decreases as the DR increases.

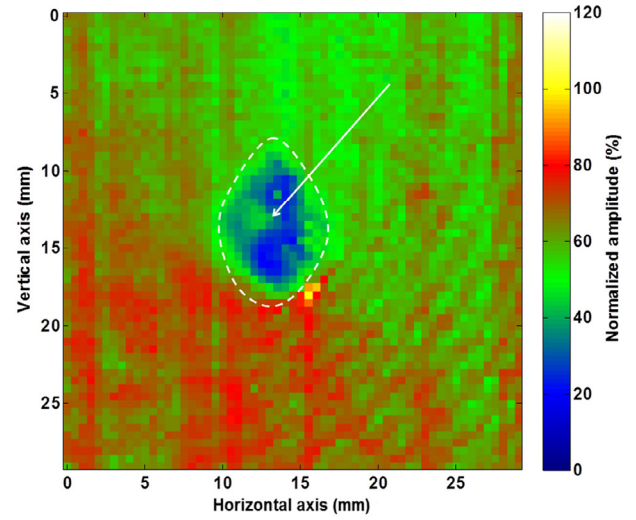

(a) THz reflection image

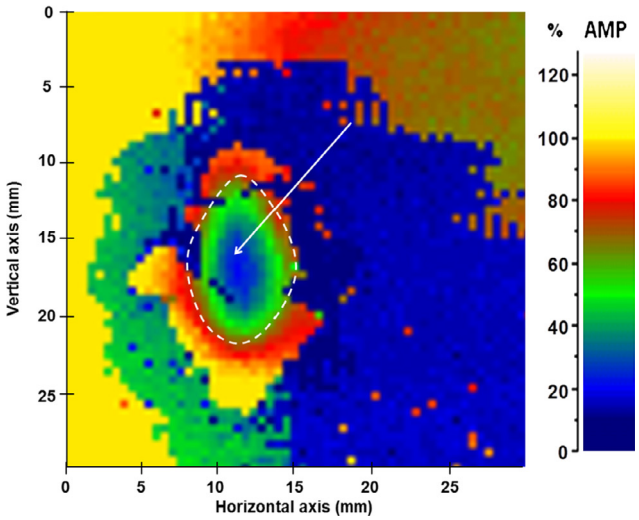

(b) Ultrasonic C-scan

Fig. 5. Sample S1 verso. (For interpretation of the references to color in this figure, the reader is referred to the web version of this article.)

Table 1
Figures of merit of the THz images.

Fig.	Test parameters	DR	SNR
3(a)	S1 refl. recto	19.2 dB	17.8 dB
4(a)	S2 refl. recto	19.2 dB	17.8 dB
5(a)	S1 refl. verso	19.4 dB	13.6 dB
6(a)	S2 refl. verso	19 dB	10.8 dB
7(a)	S1 trans.	19.8 dB	14.7 dB
7(b)	S2 trans.	19 dB	10.8 dB

4.4. Microscope observations of the damage

In order to validate our results, the two samples were cut at the impact point, perpendicularly to the crack. After polishing, the damage was observed with a Scanning Electron Microscope (SEM). Corresponding images are reported in Fig. 8.

In both cases, a crack is visible on the back side of the impact (verso) and, around this crack, a delamination zone. In picture 8(b) of damage to 20 J, it is clearly visible that the rear face of the plate is slightly convex.

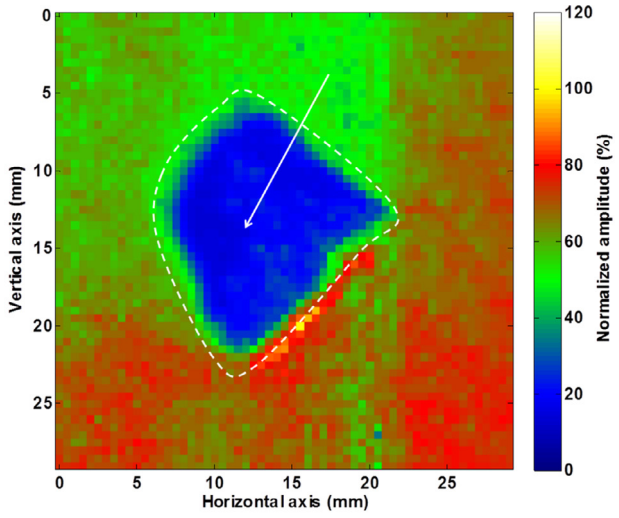

(a) THz reflection image

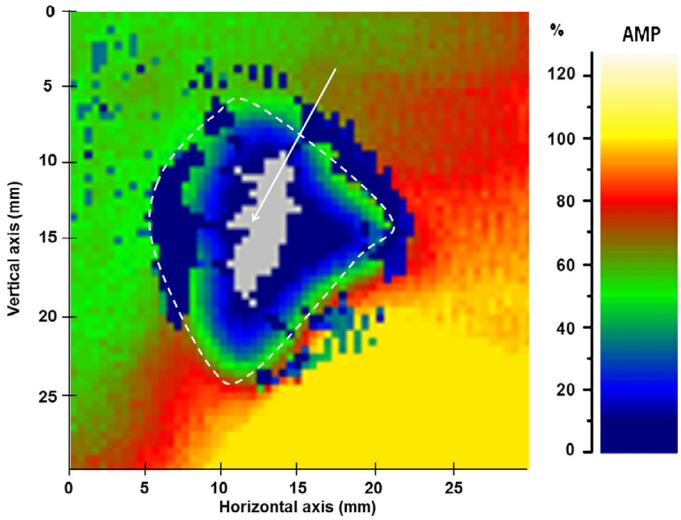

(b) Ultrasonic C-scan

Fig. 6. Sample S2 verso.

This back side curvature causes the decrease in the reflected signal and forms observed both on the THz images and on C-scan images. Weave fibers are deformed, up to delaminations. As confirmed by the 8(a) photography, plate S1, impacted at 10 J, is less damaged than S2, impacted at 20 J. The curvature of the back side is also lighter. The SEM observation shows a delamination damage ∼2 mm for the sample impacted at 10 J and about 6 to 7 mm for the second sample. The observation of the two plate cuts are in good agreement with the THz transmission images where damage widths of the same order of magnitude are observed.

5. Conclusion

Impact damage detection on composite fiber polypropylene/polypropylene plates was performed by THz imaging in transmission and in reflection. The results were compared with ultrasonic C-scan NDT, followed by microscopic observation of induced damage. The C-scan reveals damage parallel to the plate, thus delamination. In the case of unidirectional laminates, this damage is sharp and flat and as such it is easily detected by C-scan. In the case of fabrics, where the damage is more complex with cracks between pleats but also in the fold, between the two directions of weave called meta-delamination [18], the C-scan gives an indication about the damaged area but without specifying the nature and location of the damage. The THz reflection reverse side appears to give the same indication as the C-scan while the THz transmission appears to highlight the fiber cracks. The two THz imaging techniques are complementary and can provide a NDT with information about the location and type of the damage, crucial for understanding damage in composite structures.

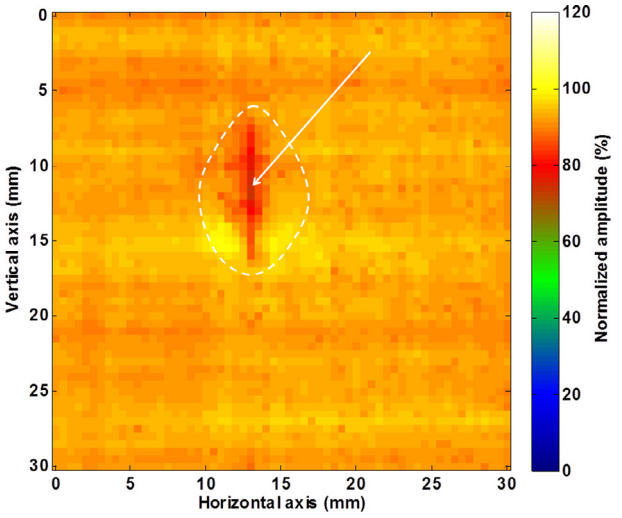

(a) Sample S1

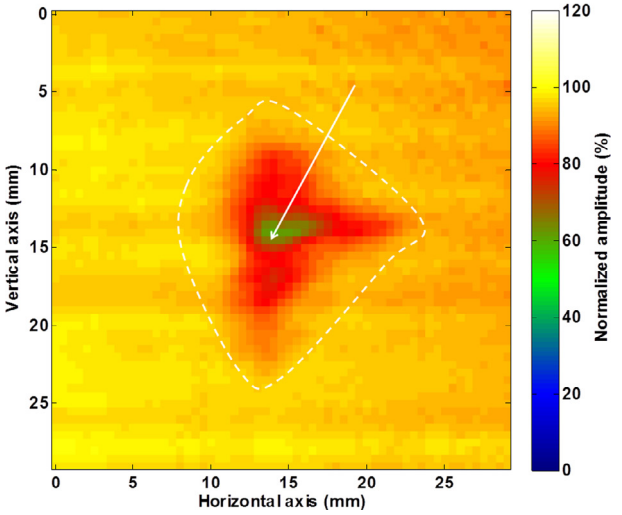

(b) Sample S2

Fig. 7. THz transmission image. (For interpretation of the references to color in this figure, the reader is referred to the web version of this article.)

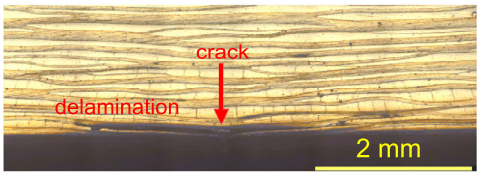

(a) Sample S1

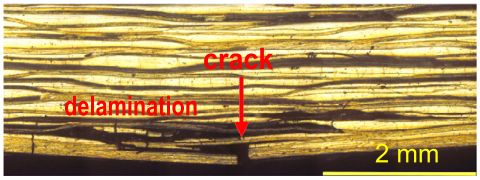

(b) Sample S2

Fig. 8. Impact damages observations with a Scanning Electron Microscope.

References

[1] Gallerano G, Doria A, Giovenale E, Messina G, Petralia A, Spassovsky I, et al. THz-ARTE: non-invasive terahertz diagnostics for art conservation. In: 33rd international conference on infrared, millimeter and terahertz waves, IRMMW-THz 2008. 2008. p. 1–2.

[2] Wietzke S, Jördens C, Krumbholz N, Baudrit B, Bastian M, Koch M. Terahertz imaging: a new non-destructive technique for the quality control of plastic weld joints. J Eur Opt Soc, Rapid Publ 2007;2:07013.

[3] Jördens C, Rutz F, Hasek T, Koch M. Towards real-time terahertz quality assurance of chocolate products. In: Joint 31st international conference on infrared millimeter waves and 14th international conference on terahertz electronics, IRMMW-THz 2006. 2006. p. 332.

[4] Jördens C, Wietzke S, Scheller M, Koch M. Investigation of the water absorption in polyamide and wood plastic composite by terahertz time-domain spectroscopy. Polym Test 2010;29(2):209–15.

[5] Zhang X-C, Xu J. Introduction to THz wave photonics, vol. 29. Springer; 2010.

[6] Rutz F, Koch M, Khare S, Moneke M. Quality control of polymeric compounds using terahertz imaging. Proc SPIE 2005;5727:115–22.

[7] Rutz F, Wietzke S, Koch M, Richter H, Hickmann S, Trappe V, et al. Non-destructive testing of glass-fibre reinforced polymers using terahertz spectroscopy. In: European conference on non-destructive testing, ECNDT2006. 2006.

[8] Jördens C, Scheller M, Wietzke S, Romeike D, Jansen C, Zentgraf T, et al. Terahertz spectroscopy to study the orientation of glass fibres in reinforced plastics. Compos Sci Technol 2010;70(3):472–7.

[9] Redo-Sanchez A, Karpowicz N, Xu J, Zhang X-C. Damage and defect inspection with terahertz waves. In: 4th international workshop on ultrasonic and adavanced methods for nondestructive testing and material characterization. 2006. www.n.net.

[10] Karpowicz N, Dawes D, Perry MJ, Zhang X-C. Fire damage on carbon fiber materials characterized by THz waves. Proc SPIE 2006;6212(1):62120G.

[11] Stoik CD, Bohn MJ, Blackshire JL. Nondestructive evaluation of aircraft composites using transmissive terahertz time domain spectroscopy. Opt Express 2008;16(21):17039–51.

[12] Ospald F, Zouaghi W, Beigang R, Matheis C, Jonuscheit J, Recur B, et al. Aeronautics composite material inspection with a terahertz time-domain spectroscopy system. Opt Eng 2013;53(3):031208.

[13] Amenabar I, Lopez F, Mendikute A. In introductory review to THz non-destructive testing of composite mater. J Infrared Millim Terahertz Waves 2013;34(2):152–69.

[14] Destic F, Petitjean Y, Massenot S, Mollier J, Barbieri S. THz QCL—based active imaging applied to composite materials diagnostic. In: 35th international conference on infrared millimeter and terahertz waves, IRMMW-THz. 2010. p. 1–2.

[15] Chassagneux Y, Wang Q, Khanna S, Strupiechonski E, Coudevylle J, Linfield E, et al. Limiting factors to the temperature performance of THz quantum cascade lasers based on the resonant-phonon depopulation scheme. IEEE Trans Terahertz Sci Technol 2012;2(1):83–92.

[16] Destic F, Petitjean Y, Mollier J. THz absolute power measurement: a simple and reliable method. In: 37th international conference on infrared, millimeter, and terahertz waves, IRMMW-THz. 2012. p. 1–2.

[17] Bouvet C, Rivallant S. Dynamic deformation, damage and fracture in composite materials and structures. Woodhead Publishing; 2016.

[18] Vieille B, Casado V, Bouvet C. About the impact behavior of woven-ply carbon fiber-reinforced thermoplastic- and thermosetting-composites: a comparative study. Compos Struct 2013;101(0):9–21.